Journal of the Indian Society of Remote Sensing
https://doi.org/10.1007/s12524-024-01900-7

RESEARCH ARTICLE

Influence of LS Factor Overestimation Soil Loss on RUSLE Model for Complex Topographies

Cristian Mejía-Parada[1] · Viviana Mora-Ruiz[1] · Jose Agustin Vallejo-Borda[1,2] · Jair Arrieta-Baldovino[3]

Received: 28 November 2023 / Accepted: 22 May 2024

Abstract
Soil loss is a crucial problem due to its importance in agricultural and livestock production, where intensive human activities have exacerbated erosive processes. In this framework, the RUSLE model emerges as a crucial tool for soil loss estimation, with the LS factor being a central component of the model. However, several research studies have shown that an inadequate selection of LS can overestimate soil erosion in complex topographies. This study assesses the overestimation of the RUSLE (Revised Universal Soil Loss Equation) model by slope length and steepness factor, focusing on a complex terrain characterized by abrupt changes in elevation and slope. Seven divergent equations were used to evaluate the LS factor and compared with the results of the RUSLE model. The findings revealed that the models proposed by Desmet and Govers and Moore and Brusch proved best suited to terrain with such characteristics, avoiding over-estimation. The meticulous selection of the LS model was highlighted as a crucial aspect, underlining the importance of an accurate methodology in soil loss measuring in topographically complex environments. This study contributes to the understanding and improvement of erosion models, providing valuable guidelines to address soil loss overestimation by LS-Factor.

Keywords Soil Loss · RUSLE · LS-Factor · Complex topography

Introduction

The combination of factors as the atmosphere, geosphere, biosphere, and hydrosphere generates solid particles of minerals from organic material, weathered rocks, and pores containing water and air (Michalopoulou et al., 2022). On the other hand, fertile soil is one of the natural resources that has benefited mankind the most over time. The application of this material in agriculture and livestock provides approximately 95% of the world's food, making it a critical natural resource for feeding a constantly growing population (Spanner & Napolitano, 2015). However, this resource is directly affected by erosive processes that have been increasing paradoxically with the increase of land dedicated to agricultural processes (Kidane et al., 2019). These losses of material are mainly generated by hydrological cycles that generate losses estimated at between 25,000 and 40,000 million tons of surface soils representing economic losses of around 400,000 million dollars due to the loss of agricultural production (Das et al., 2022; Montanarella, 2015; Spanner & Napolitano, 2015).

Considering the above, the study of erosive processes has been approached for decades, where different models have

✉ Cristian Mejía-Parada
cmejia5@udi.edu.co

Viviana Mora-Ruiz
jmora13@udi.edu.co

Jose Agustin Vallejo-Borda
JoseVallejo@tec.mx

Jair Arrieta-Baldovino
jarrietab2@unicartagena.edu.co

1 Grupo de Investigación en Amenazas, Vulnerabilidad y Riesgos a Fenómenos Naturales que Colocan en Peligro la Vida Humana y los Bienes (AVR), Programa de Ingeniería Civil, Universidad de Investigación y Desarrollo, Cl. 9 # 23-55, 680001 Bucaramanga, Santander, Colombia

2 Departamento de Tecnologías Sostenibles y Civil, Tecnológico de Monterrey, Monterrey, México

3 Programa de Ingeniería Civil, Facultad de Ingeniería, Universidad de Cartagena, Avenida del Consulado Calle 30, 48-152, 130015 Cartagena de Indias, Colombia

Published online: 11 June 2024

been proposed, which have determined rainfall intensity, soil properties, land use, soil conservation practices and topographic condition of the terrain as the predominant factors in erosive processes (Azizian & Koohi, 2021; Wischmeier & Smith, 1978). So far, different researchers have carried out mechanistic studies of soil erosion behavior as well as soil loss estimation. This has resulted in different empirical, physical and conceptual models that attempt to describe and estimate this problem (Ghosal & Das Bhattacharya, 2020; McCool et al., 1987; Mitasova et al., 1996; Moore & Burch, 1986; Smith et al. 1957; Van Oost et al., 2000). However, of all the models the best known and implemented is the RUSLE model (Revised Universal Soil Loss Equations) where its formula indicates an estimation of soil loss in tons per year, its implementation success is due to its relatively simple but robust expression in the form of estimation of soil loss increment (Xu et al., 2022).

Smith et al. (1957) determined soil erodibility (K-Factor) and soil erosivity (R-Factor) as the predisposing factors since soil properties and their interaction with rainfall intensity are the main causes of soil scouring leading to sediment displacement. However, other research has highlighted how topography is a clear predisposing factor in the behavior of the erosive process of soil (Anjitha Krishna et al., 2019; Ansari & Tayfur, 2023; Azizian & Koohi, 2021; Karásek et al., 2022; Michalopoulou et al., 2022). Within the RUSLE model, the factor describing topography is known as LS-Factor, a dimensionless variable composed of two subfactors, slope length (L) and slope steepness (S), which contribute equally to erosion. The cumulative volume and growth of runoff increases as the slope length of the land becomes steeper. As the slope increases, the flow velocity also increases, controlling erosion (Ghosal & Das Bhattacharya, 2020).

Authors like Lu et al. (2020) and Das et al. (2022) describe the slope length (LS-Factor) gradient as the most important empirical models in soil erosion estimation. However, it has also been defined that much of the uncertainty in soil loss calculation is due to exaggerate estimation of soil loss when the inadequate LS-Factor is evaluated (Wang et al., 2001). The evaluation of the LS factor has been subject to revisions with the advent of digital elevation model DEMs in soil estimation studies. The implementation of the concept of slope length in the raster environment with the use of DEMs, as well as their adjustments in the verification of slope length, may be among the major contributions in the evaluation of this factor in recent times (Anjitha Krishna et al., 2019). Despite these advances, the models still mostly follow empirical processes that do not allow generalizing the behavior of all terrains, making the calculation of the LS-Factor much more complex to estimate and generalized.

This study aims to apply the most named topographic models proposed by different authors (1) Wischmeier and Smith (1978), (2) Moore and Burch (1986), (3) McCool et al. (1987), (4) McRoberts (Renard et al., 1997), and (Desmet & Govers, 1996). This was to evaluate the relationship between the LS-Factor and RUSLE equation while the other factors (K-Factor, C-Factor, P-Factor, and R-Factor) are kept constant.

This research allows to visualize which LS factors generate lower overestimates in the RUSLE models in complex terrains, with the intention of having more realistic models of the erosive processes present. This is of vital importance in developing countries with intensive agricultural practices and without previous studies on the region. The study area is a mostly rural zone that contemplates a totally starry landscape with very large variations in terrain elevation between the east and west of the territory, with abrupt changes in topography throughout the study area. This research will help urban planners to estimate soil loss, make land management plans, and set a precedent on the importance of proper selection of the topographic model, especially on land with very starry topography in regions with similar topographies.

Material and Methods

Study Area

The study area, San Bernardo Municipality, is located in the province of Cundinamarca, Colombia, with an area of 249 km^2 (Fig. 1). This region is located between 4° 02′ N to 4° 14′ N and 74° 30′ W to 74° 14′ W. The region under study has a complex topography encompassing significant elevation variations over relatively short distances. In the eastern portion of the study area analyzed, the altitude is mainly defined by elevations ranging between 3400 and 4020 m above sea level (m.a.s.l), corresponding to the "Sumapaz Paramo". This Paramo is part of the country's central mountain range being part of the Andes Mountain. From the paramo to the west of the municipality, it decreases significantly from 3400 to 918 m above sea level (m.a.s.l.), creating a complex and rugged topography (Appendix 1). This topography configuration persists until reaching the western end of the municipality. Additionally, the urban area is located at an altitude of 1600 m.a.s.l. The region is drained by a large stream with a principal river called "Rio negro" which originates in the center of the municipality and across the region to the northwest of San Bernardo. However, because of the pronounced topographic slopes, the municipality has many streams originating in different locations and directions.

Despite Colombia being located near the equatorial line consistent with a tropical hot and humid climate, the effects of the Andes Mountains produce a wide range of climatic conditions associated with the altitudinal gradient. Climate Classification based on altitude, as the Caldas Scale mentioned that the climate of a region can divided

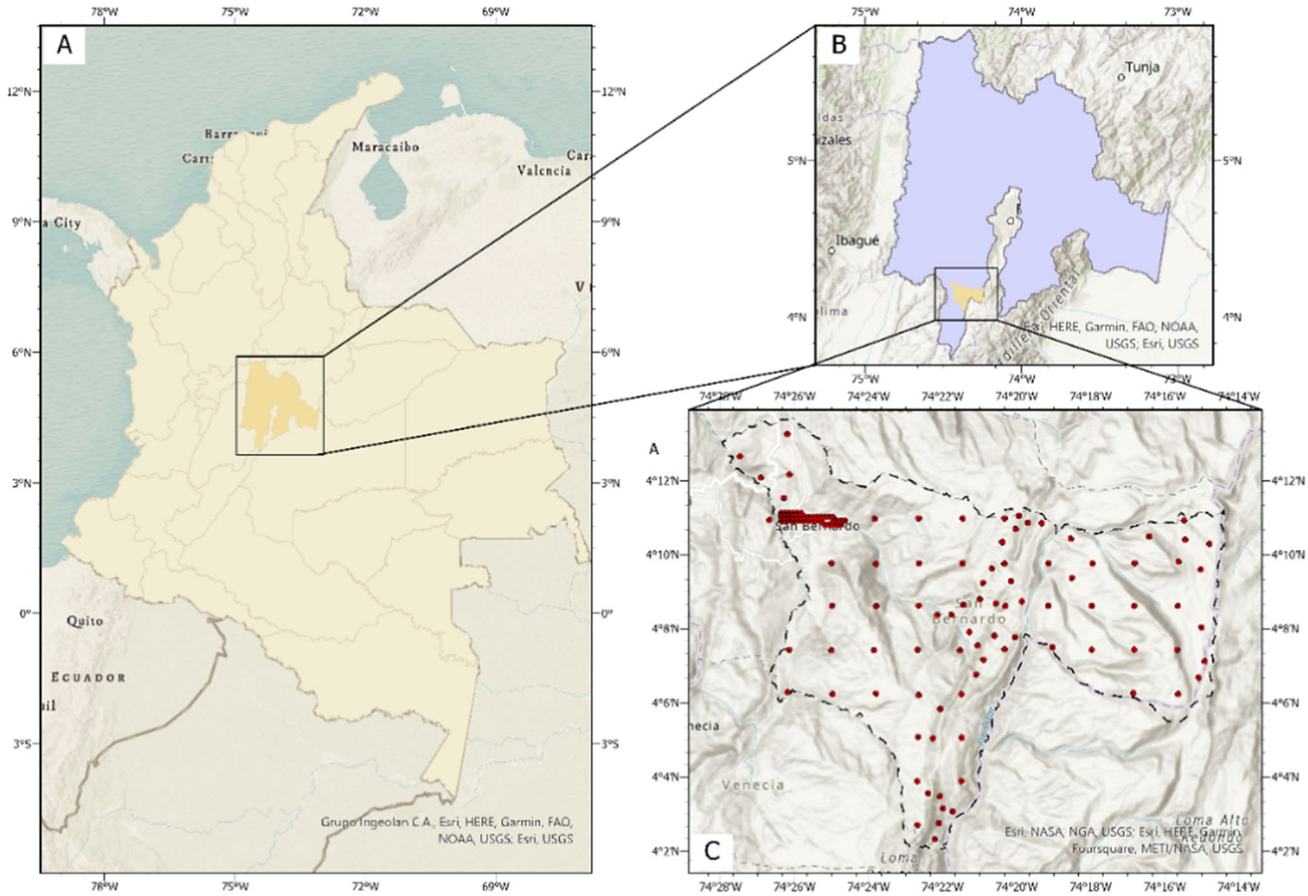

Fig. 1 San Bernardo Municipality Location. **A** Colombia Location; **B** Cundinamarca Province; **C** San Bernardo Municipality and 128 Sample location points

into hot (0–1000 m.a.s.l.), cool (1000–2000 m.a.s.l), cold (2000–3000 m.s.a.l), low Paramo(3000–3700 m.a.s.l) and high Paramo (> 3700 m.a.s.l) (IDEAM, 2023). Based on the previous statement, the study area, with mainly topographic variations along the east–west direction, allows the generation of almost all thermal floors.

As a tropical country, Colombia has a wide range of precipitation ranging from arid zones with precipitation less than 375 mm/year to super humid zones with an impressive 15,000 mm/year (IDEAM, 2023). In this context, the study area ranges between 500 mm/year and 1450 mm/year, which will be described in more detail in more advanced stages of the research.

Due to the significant change in climatic conditions associated with elevation, precipitation, and economic activities, San Bernardo presents various land uses, among which the urban area, the agricultural zone, the peninsular forest, paramo, sub-paramo, and areas for waste disposal stand out. The main economic activity in the region is based on agriculture, including different types of crops and natural pastures dedicated to livestock. Also, the region includes undisturbed forests located all over the Municipality. However, due to the significant steep slopes, bare land is in the center and east of the territory.

Data Collection

The study used spatial datasets from different sources to represent the topography and vegetation. Regarding rain data, 11 pluviometry stations from the IDEAM (Instituto de Hidrologia, Metereología y Estudios Ambientales) which cover the study area with information from 2012 to 2022 were used to analyze the updated rainfall trend. The compilation of all datasets and data collected is presented in Table 1. On the other hand, for soil structure data, 128 samples were taken in the field (Fig. 1). The collected samples were subjected to the following tests: moisture content, particle size determination using a granulometry and hydrometer, liquid limit, plastic limit, and organic matter content by ignition.

Methods

The spatial distribution of all the factors involved in the RUSLE model was carried out in a GIS platform using the

Table 1 Spatial datasets used for the LS-factor and RUSLE modeling

Datasets/data collection	Data source
DEM*	ALOS PALSAR 12.5 m DEM* https://search.asf.alaska.edu/#
NDVI+	Alaska Satellite Facility Distributed Active Archive Centers (ASF DAAC) GEE+++ Landsat 8 Dataset Imagery (30 m) https://developers.google.com/earth-engine/datasets/catalog/landsat-8 A product of GEE and NASA
Rainfall Data	consultation and downloading of hydro-meteorological data http://dhime.ideam.gov.co/atencionciudadano/ A product of IDEAM∞

*DEM, digital elevation model; +NDVI, normalized difference vegetation index; ∞IDEAM, Instituto de Hidrología, Metereología y Estudios Ambientales

+++Google Earth Engine Platform

WGS1984 datum as a spatial reference, according to the process shown in Fig. 2. RUSLE was designed to present the mean annual soil loss for ground slopes flow convergence/divergence that can be neglected, i.e., planar slopes, common in agricultural lands (Menasria et al., 2022); the RUSLE model is expressed on Eq. 1,

$$A = K * R * C * P * LS \tag{1}$$

where A = soil loss (ton ha − 1 yr − 1), K = soil erodibility (ton h MJ − 1 mm − 1), R = rainfall erosivity factor (MJ mm ha − 1 h − 1 yr − 1), C = land management factor (dimensionless), and P = conservation practice factor (dimensionless), and LS = slope-length and slope steepness factor (dimensionless) (reference).

RUSLE Parameters Computation

Soil Erodability Factor (K-Factor) The K factor is defined as the relationship between soil loss due to the soil structure and external factors such as rainfall, and its values are usually categorized in a range from 0 to 1 depending on the type of managed measure units (Brahim et al., 2020). The importance of soil as an erosion factor lies in its capacity to infiltrate and transport water through the soil, which has been formed through geological, climatic, temporal, and anthropological processes (Dam Nguyen et al., 2022).

There are many equations for calculating the soil erodibility factor K (Alexandre Ayach et al., 2015; Aouichaty et al., 2022; Escobar Quintero & Macas Espinosa, 2021; Ganasri & Ramesh, 2016; Ghosal & Das Bhattacharya, 2020; Wischmeier & Smith, 1978). However, this study used the Eq. 2 (Mohammed et al., 2020),

where, SAN is %sand, SIL is % silt, CLA is %clay, OM is %organic matter, and SN1 = 1-SAN/100. The percentage of silt, sand, clay, organic matter, structure code, and permeability of the soil material in the 128 samples collected in the study area were determined using the American Association of State Highway and Transportation Officials (AASHTO) classification system, Unified Soil Classification System (USCS) and correlations based on typical values of their characteristics. Manual calculation of the K-Factor value for each sample was carried out, and the results were interpolated using the inverse weighted distance (IDW) method within the GIS platform. With this tool, the original values of the points could be better preserved due to the extension of the terrain.

Rainfall Erosivity Factor (R-Factor) Soil loss is directly related to rainfall energy and intensity. This last point is relevant since heavy and frequent rains can generate runoff that accelerates erosive processes. In contrast, soft and spaced rains allow better soil infiltration, reducing the probability of soil erosion (Zhou et al., 1995). Different equations have been created to assess how rain affects soil loss (Bols, 1978; Fayas et al., 2019; Ganasri & Ramesh, 2016; Mohammed et al., 2020; Sinshaw et al., 2021; Zhou et al., 1995). Nevertheless, the equation selection depends on the available data, climate, and the geographic location (Ghosal & Das Bhattacharya, 2020). This study collected monthly precipitation data from IDEAM for the last ten years from the 11 meteorological stations closest to the study area as mentioned before. The equation integrated to generate was the Fornier Modified Index FMI (Eq. 3) used previously in other studies with similar rainfall behav-

$$K = \left(0.2 + 0.3e^{\left(-0.0256SAN\left(1-\frac{SIL}{100}\right)\right)} * \left(\frac{SIL}{CLA + SIL}\right)^{0.3} * \left[1 - \frac{0.25OM}{CLA + e^{(3.72-2.95OM)}}\right] * \left[1 - \frac{0.75N_1}{SN_1 + e^{(22.9SN_1-5.51)}}\right]\right) \tag{2}$$

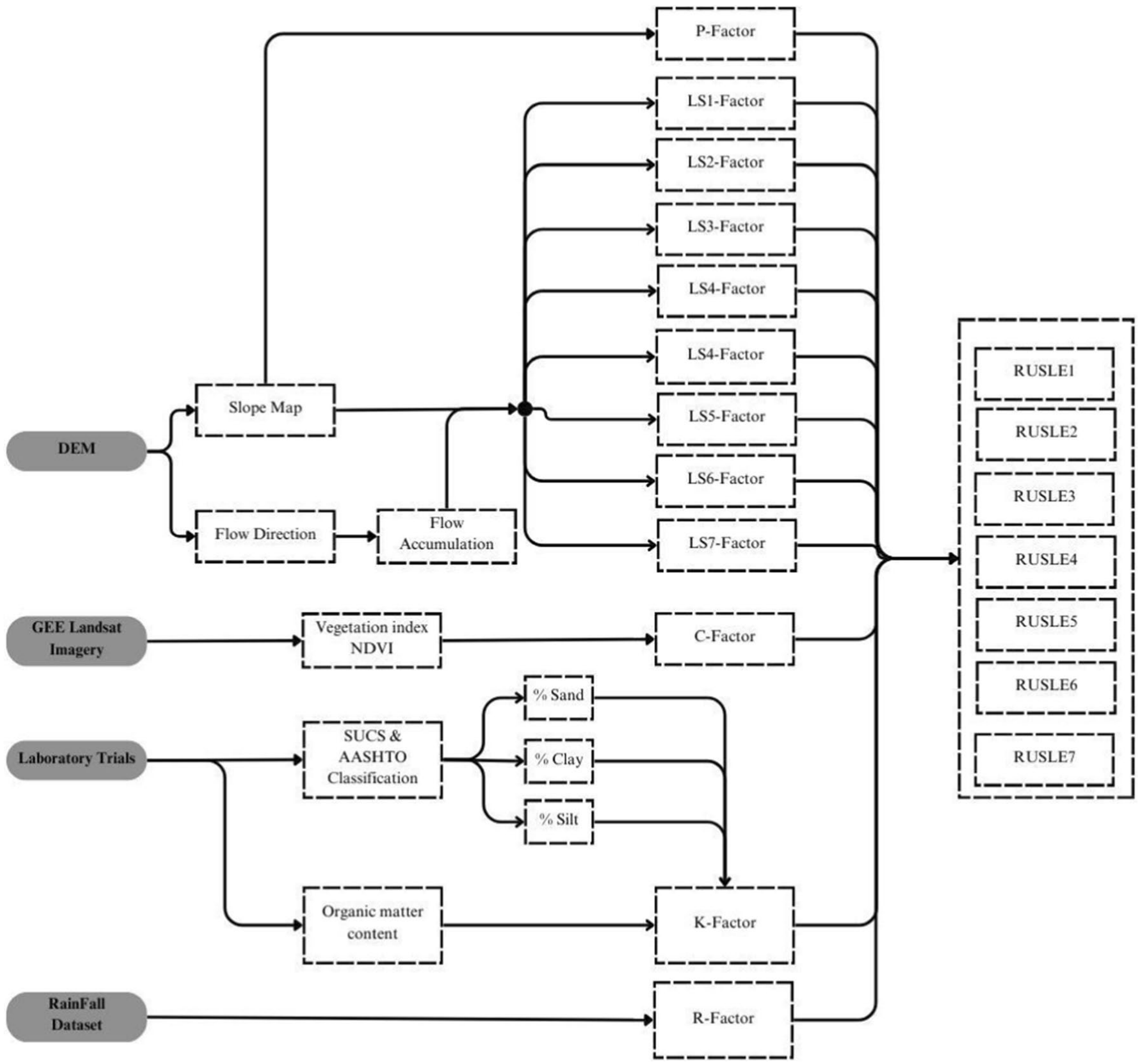

Fig. 2 Methodological framework of implementing LS-Factor and RUSLE model for the soil erosion comparison

ior (Arnoldus, 1977; Brahim et al., 2020; Ganasri & Ramesh, 2016).

$$R = \frac{\sum_{i=1}^{12} Pi^2}{\sum_{i=1}^{12} p} \tag{3}$$

where, Pi is the monthly rainfall (mm), and p is the cumulative annual rain data, for the interpolation IDW tool was implemented due to the limited number of points that evaluated the zone.

Cover Management Factor (C-Factor) The land management C-Factor is an important parameter in evaluating soil erosion, as it represents the surface of the vegetation and the control measures of soil erosive factors. The vegetation cover protects the land from progressive erosion generated by natural or external factors; the range goes between 0 to 1, where close values to 0 indicate a well-protected land area (Jazouli et al., 2019; Mohammed et al., 2020). With the current availability of high-quality satellite images from space missions, bands interpretation has implemented for model C-Factor. For example, the NDVI index, which represents the measure of greenness and density of the vegetation captured in an image had been proposed as an efficient way to represent the C-Factor (Durigon et al., 2014; Hui et al., 2010; Mallick et al., 2014). The current study took the Eq. 4 previously used on tropical regions (Durigon et al., 2014).

$$NDVI = \frac{NIR - RED}{NIR + RED}\ C = \frac{-NDVI + 1}{2} \tag{4}$$

where NIR is a nearly the infrared band, and RED corresponds to the red color band, both bands from the Landsat 8 imagery, NDVI is the normalized difference vegetation index, and C is the C-Factor.

Table 2 P-Factor for slope as per agricultural practice (Wischmeier & Smith, 1978)

Percentage of land slope [%]	*P*-value
1–2	0.6
3–5	0.5
6–8	0.5
9–12	0.6
13–16	0.7
17–20	0.8
21–25	0.9
> 25	1.0

Support Practice Factor (P Factor) The factor of conservation practices P indicates the management practices aimed at reducing soil erosion. Conservation practices aim to minimize the amount of erosion on a piece of land, and the P-Factor is used to reflect the material loss concerning a particular conservation practice, such as farming, terracing, alley cropping, cross-slope crops, and watercourses (Ghosal & Das Bhattacharya, 2020; Qiankun et al., 2019). The P factor is expressed on a scale from 0 to 1, with values closer to 1 representing the absence of conservation practices and values closer to 0 indicating the presence of effective conservation practices, such as planting crops in contours or urban areas (Koirala et al., 2019). For the study, considering that the proposed land is dedicated as farmland, an agricultural support practice design by Wischmeier and Smith (1978) was chosen (Table 2).

LS-Factor Models

Topographic factor LS-Factor includes sub-factors known as slope-length (L) and slope steepness factor (S), which can be determinate with a DEM. Because of the inclination and slope length of the terrain, the soil loss increases as the slope length increases (Ghosal & Das Bhattacharya, 2020; Schmidt et al., 2019). Several authors worldwide have developed different expressions to evaluate the L and S subfactors in soil loss estimation. For this study, seven approaches for topographic LS-Factor were adopted. The models include similar expressions for the L and S factors; these subfactor combinations were made based on the equations presented by authors and their experiences with those models. The equations were taken from the review made by Ghosal and Das Bhattacharya (2020) during its review of the RUSLE model. During this brief, the author compiled

Table 3 LS-Factor expressions were evaluated in the study (Ghosal & Das Bhattacharya, 2020)

Method	Authors	Expression	Description	Equation
LS1	Wischmeier &Smith	$LS = \left(\frac{\lambda}{22.13}\right)^m .(65.41 sin^2\theta + 4.56\sin\theta + 0.065)$	Where λ is the slope length in (meters), and m is equivalent to 0.5 for slopes steeper than 5%, 0.4 for slopes between 3 and 4%, 0.3 for slopes between 1 and 3%, and 0.2 for slopes less than 1%	(5)
LS2	Moore & Brusch/ Mitasova	$LS = \left(\frac{\lambda}{22.13}\right)^m \left(\frac{\sin\theta}{0.0896}\right)^n$	Where, coefficiente m and n varies in diferents studies. LS2 (m = 0.4; n = 1.1), LS3 (m = 0.4;n = 1.3), and LS4 (m = 0.6;n = 1.3)	(6)
LS3				
LS4			Where θ represents the slope in degrees; however, it usually has to be converted into radians in the GIS platform	(7)
LS5	McCool, Foster, Weesies	$LS = \left(\frac{\lambda}{22.13}\right)^m$ $m = \frac{(sin\theta/0.0896)/[3x(sin\theta)0.8+0.56]}{1+(sin\theta/0.0896)/[3x(sin\theta)0.8+0.56]}$ $S = \left\{\begin{matrix} 10.8 sin\theta + 0.03\theta < 5° \\ 16.8 sin\theta - 0.55° \leq \theta \geq 10° \\ 21.9 sin\theta - 0.96\theta \geq 10° \end{matrix}\right\}$	Where, m represents the ratio of rill to inter-rill erosion	(8)
LS6	McRoberts	$LS = \left(\frac{\lambda}{22.13}\right)^m$ $m = \frac{(sin\theta/0.0896)/[3x(sin\theta)0.8+0.56]}{1+(sin\theta/0.0896)/[3x(sin\theta)0.8+0.56]}$ $S = \left\{\begin{matrix} 10 sin\theta + 0.03\theta < 9° \\ 16.8 sin\theta - 0.55 \geq 9° \\ - \end{matrix}\right\}$		(9)
LS7	Desmet & Govers	$L_{ij} = \frac{(A_{ij-in}+D^2)^{m+1} - A_{ij-in}^{m+1}}{D^{m+2x} X_{ij}^m x22.13^m}$	Where $A_{(i,j)}$ is the contributing area at the inlet of the grid $cell_{(i,j)}$ measured in m^2, D is the grid cell size (meters), x = sin $a_{i,j}$ + cos $a_{i,j}$, the $a_{i,j}$ is the aspect direction of the grid cell $_{(i,j)}$	(10)

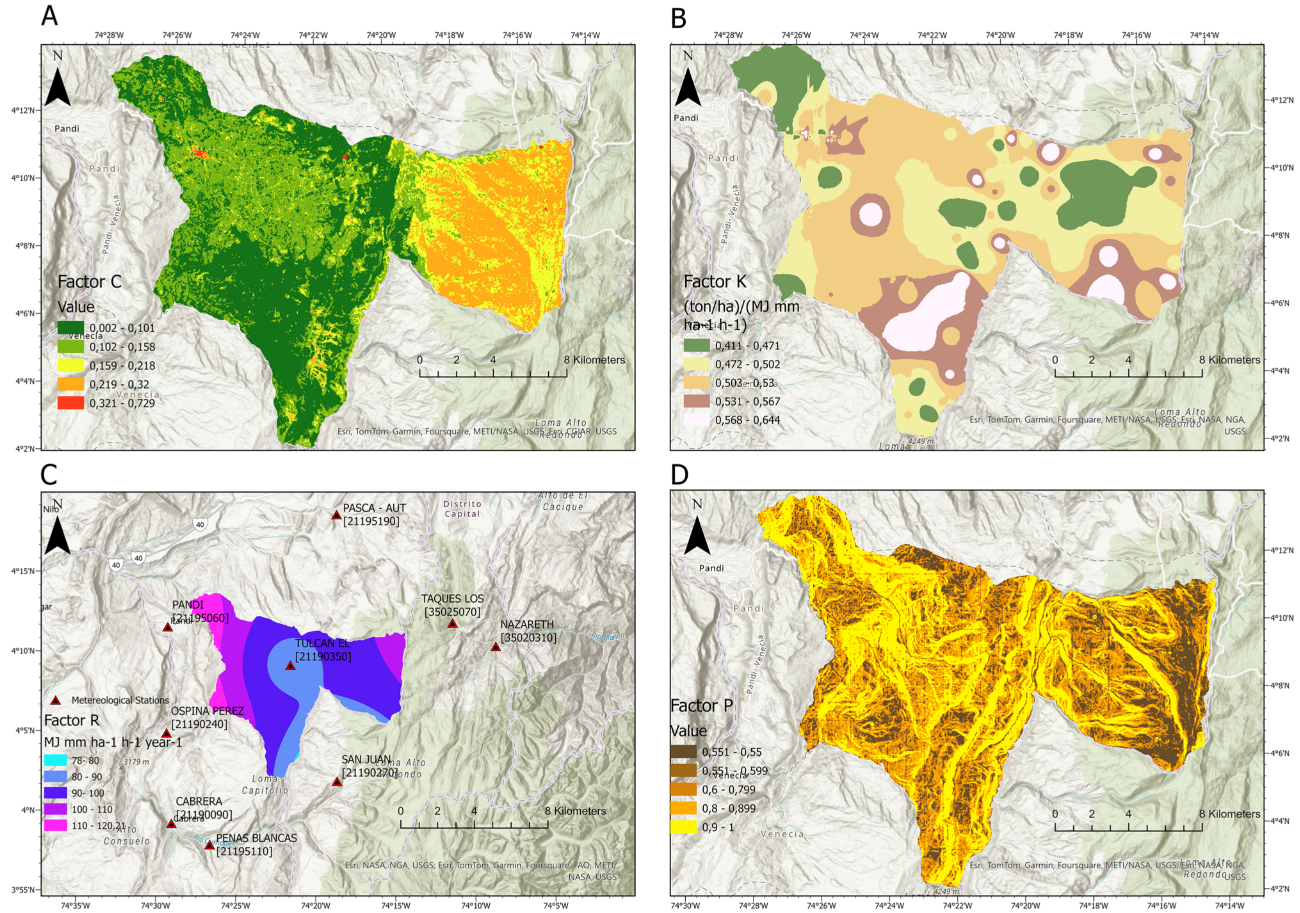

Fig. 3 RUSLE general Factors. **A** C-Factor; **B** K-Factor; **C** R-Factor; **D** P-Factor

the most common algorithms implemented for evaluating LS-Factor, presented in Table 3.

In most of the selected expressions (Except LS7), the evaluation of the relative slope length (L-Factor) has the same structure where the flow path length (λ) is related to a basic slope length of 22.13 m. This λ is denoted as λ = (flow accumulation x DEM´s cell size). However, other researchers as Das et al. (2022) have indicated that in basins with large land extensions and steep slopes, it is a mistake to contemplate λ in this way because it generates exaggerated overestimates of the factor L. Therefore, for the study, all the expressions, which include λ, were modeled based on alternative lambda evaluation to ensure the reduction of the overestimation by the slope length factor presented in Eq. 11.

$$\lambda = \frac{\Delta H}{\sin\left[\tan^{-1}\frac{\Delta H}{I_o}\right]} \tag{11}$$

where Io is the distance between each point and the grid. ΔH is the height difference between the maximum and minimum pixel, obtained by applying ΔH = tan A * I_o. A is the digital model of slope in degree.

Results and Discussion

Rusle factors Modeling

From the equations mentioned before, were obtained the spatial distribution for the factors K, C, R and P shown in Fig. 3. All of them were process on the GIS platform using the dataset collection (Table 1). Figure 3 illustrates how Factor-C exhibits dense vegetation in the central and northwestern areas of the study area, in line with the forested regions and areas dedicated to agriculture in this region. Likewise, a red area is observed in the northwestern part, which coincides with the urban core of the territory. On the eastern side, there are yellow areas that denote land devoid of vegetation, associated with the increase in terrain altitude and the presence of the Sumapaz paramo. Regarding the K-Factor, a variability in erodibility processes linked to soil type is identified, highlighting a decrease in infiltration and a potential increase in erosion to the south of the study area. On the other hand, the R-Factor, related to precipitation in the area, indicates that the areas to the south present lower rainfall intensity values, which reduces erosive processes in this parameter. However, it is evident how the values of potential water erosion extend towards the eastern and western sides. Finally, the P-Factor confirms the complex topography of the region studied, showing that the furrows in areas with dense vegetation and in land used for agricultural activities show values close to 1.0, which indicates a potential increase in erosion due to insufficient conservation practices applied in this type of relief.

The conditions of the four factors previously mentioned were kept constant in each of the 7 comparison models of the LS Factor, with the purpose of evaluating the influence of this factor in the model, keeping the other parameters of the equation equally.

Annual Soil Loss Comparison

Annual soil loss for the study area was estimated by acquiring the Revised Universal Soil Loss Equation and multiplying the erosion potential factors together with the LS models. Seven estimation models were obtained in the process and were named by the same numeration present for the Slope Length and Steepness Factor (LS) described previously in Table 3. From this process, seven maps of soil erosion were produced using the RUSLE model with the different LS-Factors proposed. The results are presented in Fig. 4, 5 and 6, shown the Slope and Steepness factor in the left map and the RUSLE soil loss map on the right for each ran model.

From the LS-Factors the most significant difference is associated with evaluating the S factor. This is because the reference authors have assessed the slope steepness with linear, quadratic, and exponential models based on slope percentages of their study regions that not always represent different terrains, limiting the ability to assess complex terrain. On the other hand, the L factor, in most authors, tends to be estimated following the initial premise implemented by Wischmeier and Smith (1978), where the concept of slope length related to the accumulation flow and the pixel size of the digital elevation model is used. Even so, it has been found that the traditional lambda relationship can generate overestimates (Anjitha Krishna et al., 2019; Das et al., 2022), especially in complex terrains that generate high accumulations along hydrological basins. Only the researchers Desmet and Govers (1996) proposes a significant modification of the L factor (LS-7). They include the form of convergence or divergence between the accumulation flow and the terrain pixel.

LS-Factor and RUSLE Statistics

The descriptive statistics were calculated based on each LS-Factor and RUSLE raster image generated on the GIS platform (Table 4). The LS-1 (max. 202.894) and LS-7 (max. 182.65) factors show significant maximum values concerning the other models. However, the standard deviation of the LS-7 models, with a value of 8.347, is considerably lower compared to LS-1, the latter being the highest with a value of 16.276. Also, despite having the second highest rank the LS-7 model has the lowest mean of all the models with a value of 3.536. On the other hand, LS-2 shows a statistical behavior with a higher clustering of the data than the other models, having the lowest standard deviation. For models LS-3 and LS-4, which are variations of

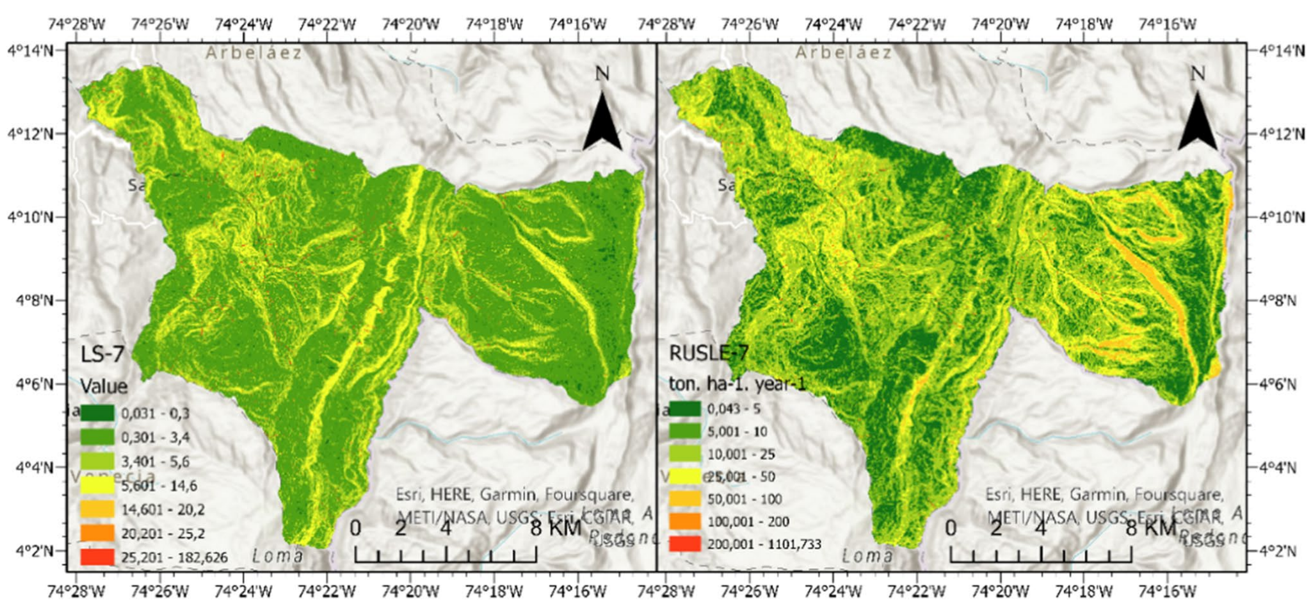

Fig. 4 LS-Factor versus RUSLE models (part 1)

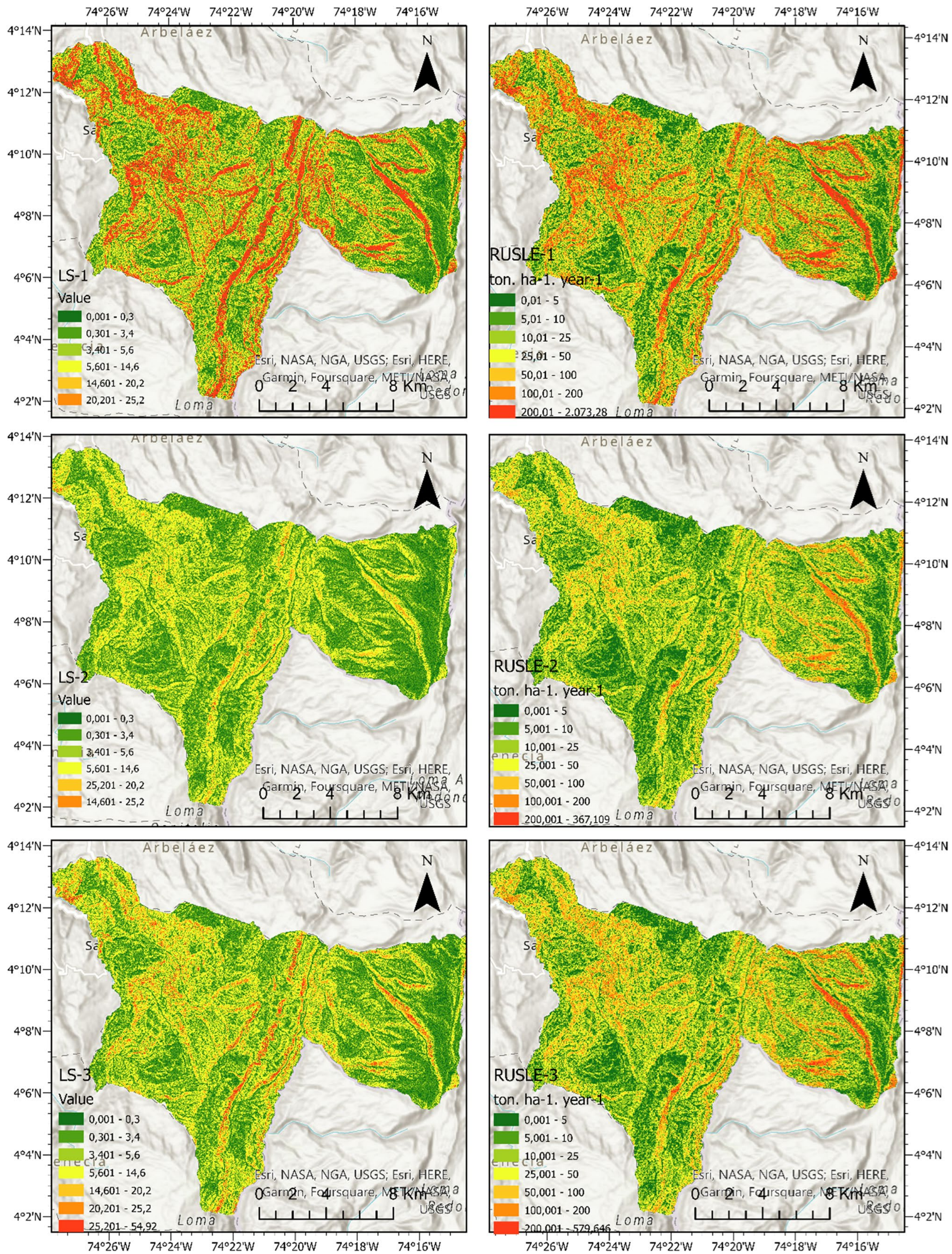

Fig. 5 LS-Factor versus RUSLE models (part 2)

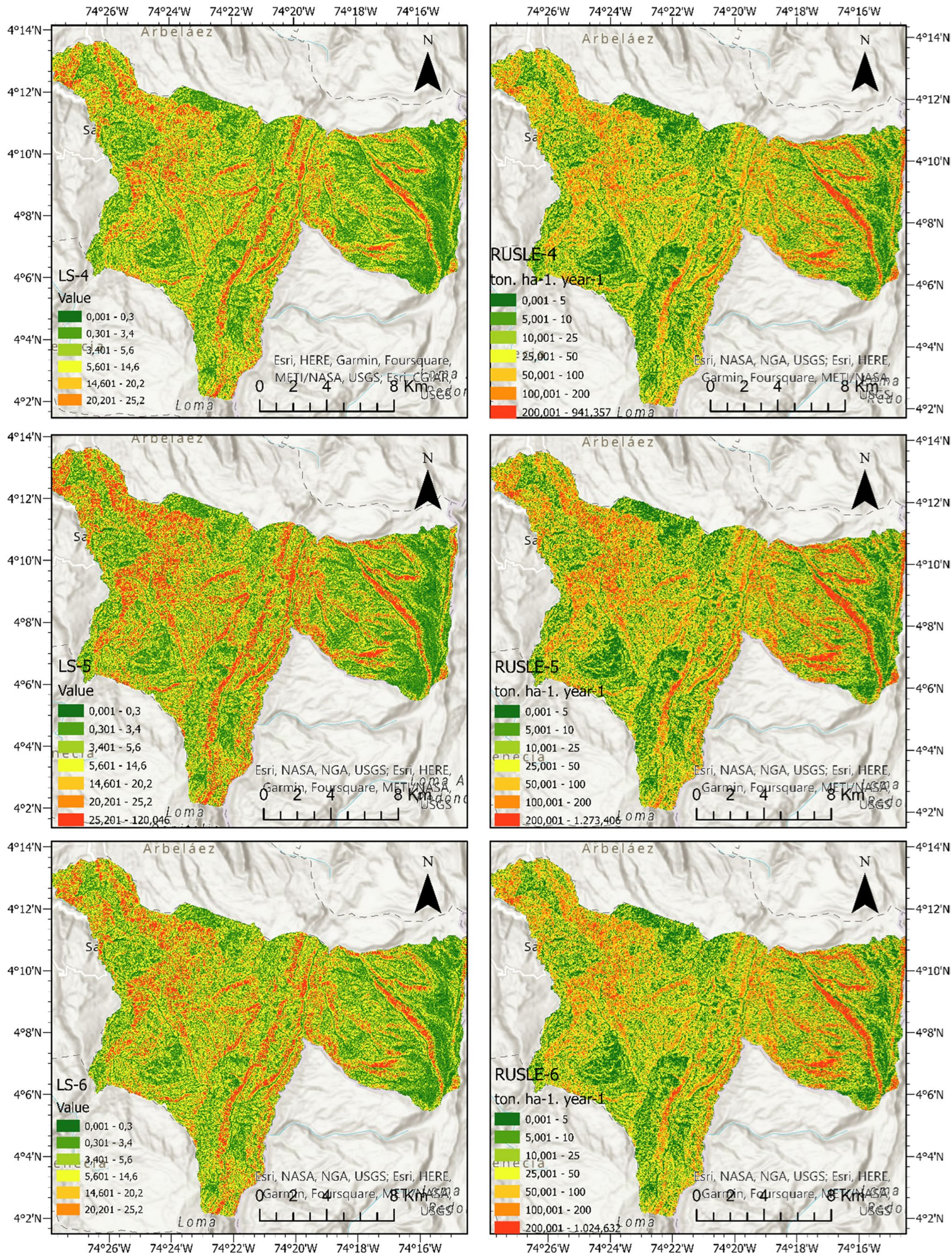

Fig. 6 LS-Factor versus RUSLE models (part 3)

Table 4 Descriptive statistics of LS-Factor models

Statistics	LS-1	LS-2	LS-3	LS-4	LS-5	LS-6	LS-7
Mean	12.583	4.869	6.366	8.785	11.035	10.038	3.536
Max	202.894	34.425	54.920	89.191	120.046	96.356	182.65
Min	0	0	0	0	0	0	0.03
Std	16.276	4.520	6.402	9.813	13.318	11.163	8.347
Range	202.894	34.425	54.920	89.191	120.046	96.356	182.626

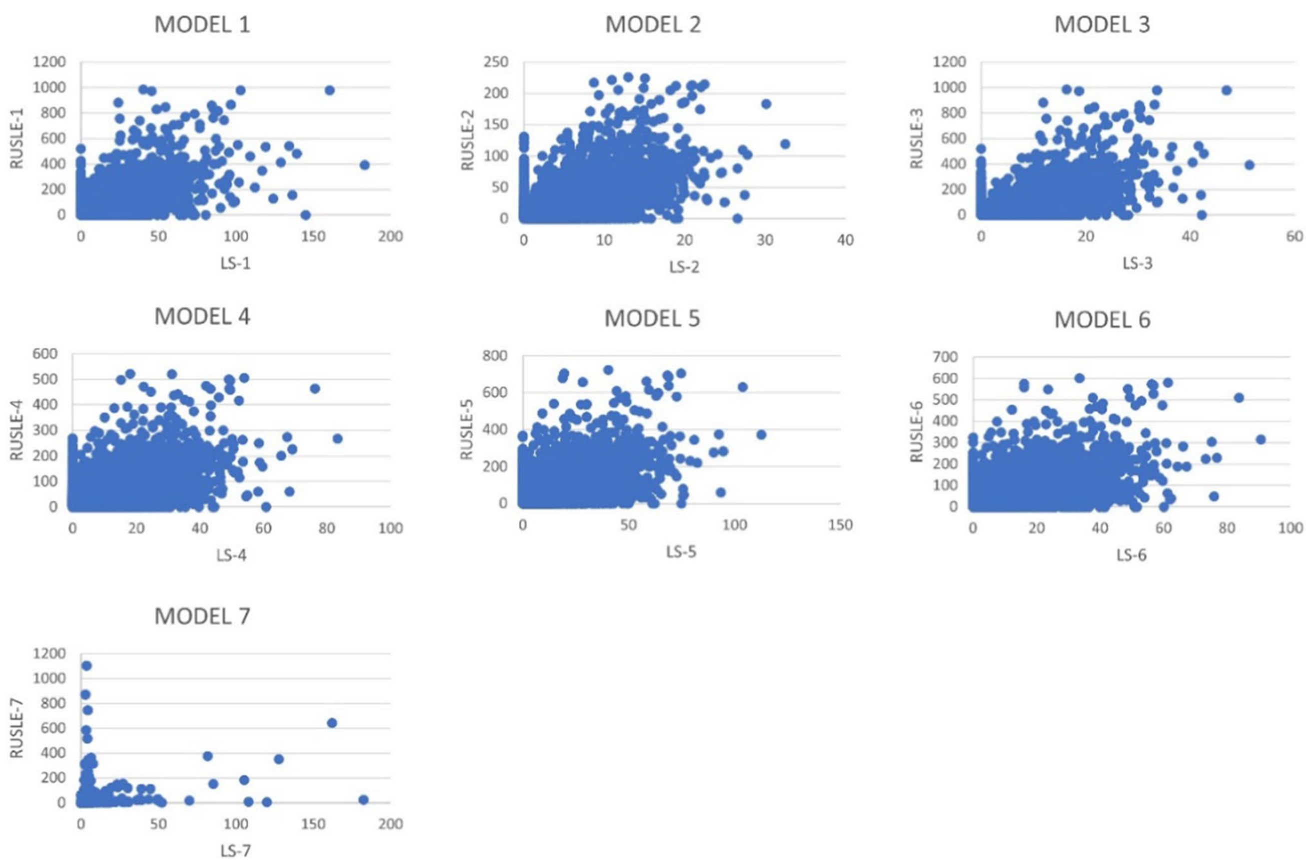

Fig. 7 Relation between LS-Factor and RUSLE soil loss estimation for each model

Table 5 The descriptive statistics of the annual soil loss for each model

Statistics	RUSLE-1	RUSLE-2	RUSLE-3	RUSLE-4	RUSLE-5	RUSLE-6	RUSLE-7
Mean	64.346	24.585	32.143	44.319	55.825	49.663	17.079
Max	2073.280	367.109	579.646	941.358	1273.406	1024.632	1101.780
Min	0.010	0.001	0.001	0.001	0.001	0.001	0.047
Std	99.311	28.551	40.088	60.018	80.473	67.681	30.643
Range	2073.270	367.108	579.645	941.357	1273.405	1024.631	1101.733

model 2, the modification of the coefficients m and n significantly impacted the growth of the LS-factor values and even increased the dispersion of their values. However, models LS-5 and LS-6 have averages like LS-1, being these three models the ones that handle higher estimates of the LS-Factor. Considering the adopted model, the two reasons that can support this behavior are: The S-factor in the three models contemplates a linear behavior that can be included in low slopes but does not allow for adequate modeling of the behavior of complex terrain with abrupt slope changes. Second, the model consists of the first estimations of lambda, which can influence the over-estimation of data.

Table 5 shows the descriptive statistics for the soil loss estimation models. Consistent with the results of the LS models, the RUSLE-1 and RUSLE-7 models show the highest values and ranges concerning the other approaches. However, RUSLE-7 has the lowest mean on soil erosion models being approximately 47 points lower than RUSLE-1. The other models maintained the same behavior shown on LS-Factor assessment, this reflects once again that the slope and steepness factor is a predominant factor on soil loss estimation models. The statistics also reflects that RUSLE-1 and RUSLE-2 are better grouped than other models, despite of that is a great difference between the range of those models.

LS-Factor and RUSLE Behaviour Comparison

Figure 7 shows that despite the statistics of each model revelated strong relations between LS and soil loss estimation, there is not a lineal regression between those variables. Otherwise, the most relevant aspect of the graph is presented in model 7, showing how the concentration of soil loss occurs at the lowest values of the LS factor, which is consistent with the statistics previously mentioned. However, it offers considerably higher outliers not seen in the other models. The explanation for this behavior must be influenced by the approach of the L factor, in which, unlike the other models, the total accumulation flow was taken and not the variation included in the lambda estimations. It is taking the above into account and visualizing the maps presented in Fig. 4. A clear significant increase in the LS values over the riverbeds is consistent with the accumulation flow. On the other hand, for the other models, similar behavior can be seen in the relationship between LS and RUSLE, considering that the growth in the RUSLE scale is much higher in models LS-1, LS-3, LS-5, and LS-6 (Table 5).

From the results presented in Fig. 4 and Fig. 7 it can be said that models 2 and 7 show the lowest soil loss estimates. However, the representation of the LS-2 factor is significantly different from LS-7. In model 2, the highest values of the LS factor are displayed in the steepest furrows of the terrain consistent with the slope map (Appendix 1). On the other hand, the LS factor in model 7 represents its highest values in the runoff zones consistent with the accumulation flow of the studied area.

Although all models share similarities in the way the L and S sub-factors are evaluated as previously mentioned, models LS1, LS3, LS4, L5 and LS6 are the ones that generate higher averages that when interacting with the other factors that compose the RUSLE equation generate overestimates for the entire terrain regardless of the slope structure of the terrain. Considering the behavior of these models and that the subfactor S is different in these models, it can be mentioned that the evaluation of factor L is the one that is generating these overestimates. This shows once again that the evaluation of the accumulation flow is not adequate in terrain with very complex topography because it does not allow modeling the abrupt or smooth changes of a terrain such as that of the area studied.

Conclusions and Perspectives

The object of this research is to examine the connection between one of the most significant parameters of the RUSLE model, such as the LS factor it is, evaluating different researcher's expression, visualizing which one best fits the study area. This assessment demonstrates that the methods to estimate the upper slope length and slope inclination are the LS-2 and LS-7 models due to the decrease in overestimation generated by conservative factors derived from the LS-1 model proposed by Wischmeier and Smith (1978). While the LS-2 model still handles the traditional lambda format, it has a modification in the modeling of the S subfactor, which no longer includes a linear behavior. However, it demonstrates the importance of the m and n coefficients in the description of a complex terrain. Although LS3 and LS-4 share the same equation as LS-2, it was found that values for $m = 0.4$ and $n = 1.1$ are enough to describe the behavior of LS without generating excessive overestimations in the algorithm in complex terrains. On the other hand, although the LS-7 model has overestimates at specific points, they are justified by the previously mentioned use of the total accumulation flow. However, despite this, the model shows less aggressive behavior in areas where there are no tributaries despite complex terrain and high slopes showing a better adaptation to sudden changes in slope length compared to other methods, focusing on natural drainage as a means of sedimentation transport.

The study also reveals the importance of adequate selection in the soil loss evaluation factor. The incorrect selection of the terrain evaluation expression leads to exaggerated results that do not allow the terrain to be modeled. The above leads to problems in data analysis, especially in regions where there are no previous studies, as is the case in the study area. The results demonstrate that in regions with very complex terrain the evaluation of subfactor L is essential to avoid overestimations. Likewise, the modeling of subfactor S following the exponential model proposed by Moore and Burch (1986) can contribute to overestimates of soil loss in a field to be evaluated.

Appendix 1. Complementary Maps

See Fig. 8

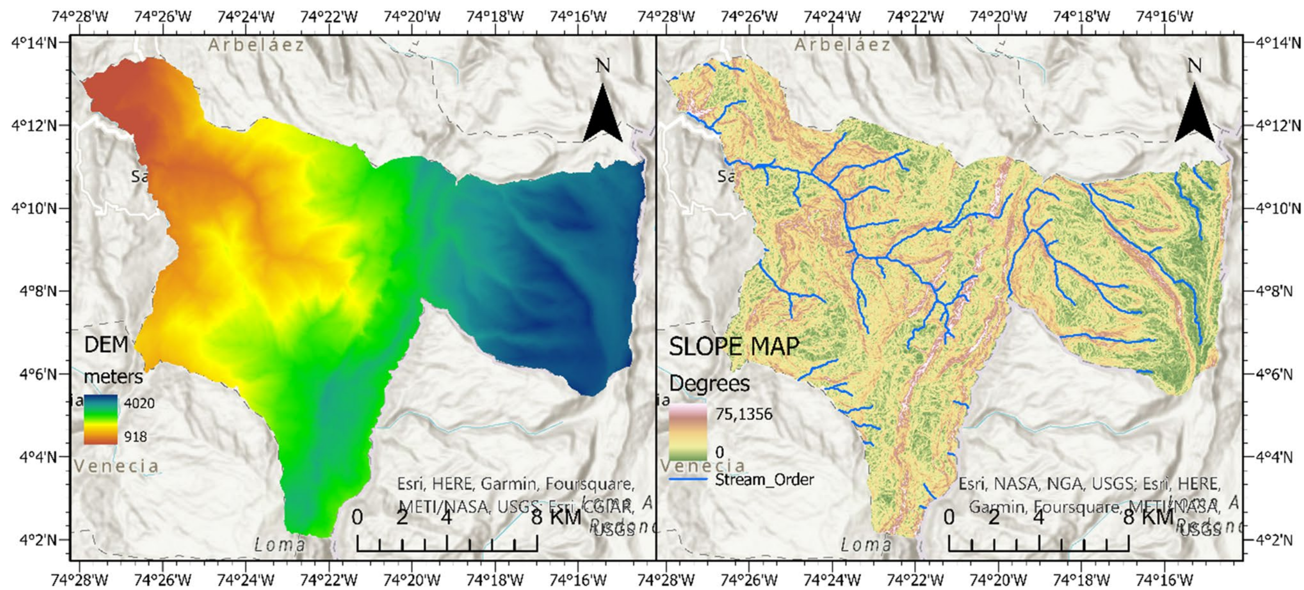

Fig. 8 DEM of Study area (Left) & Slope Map (Right)

Acknowledgements The authors would like to thank the University of Research and Development (UDI) for the support provided to develop this research. We thank the Geotechnical Laboratory for using the equipment for testing and data collection.

Author's Contribution Cristian Mejía-Parada: Conceptualization, Methodology, Draft preparation, Visualization, Data curation, Formal analysis, investigation. Viviana Mora-Ruiz: Conceptualization, Supervision, Methodology, Writing- Original, Validation, Visualization, Resources, Draft preparation, Review and Editing. Jose Agustin Vallejo-Borda: Data curation, investigation, Draft Preparation, Review, and Editing. Jair Arrieta-Baldovino: Data curation, investigation, Draft Preparation, Review, and Editing.

Funding The authors state that there is no significant financial support from any entity or individual.

Declarations

Conflict of interest The authors declared that this article is an original andunpublished work and is not being considered for publicationelsewhere. The authors declared no conflict of interestrelated to this work. The manuscript has been reviewed andapproved by all authors listed, and all authors are listed.We also confirm that all agreed to our manuscript's authors'order.

References

Anache, J. A. A., Bacchi, C. G. V., Panachuki, E., & Sobrinho, T. A. (2015). Assessment of methods for predicting soil erodibility in soil loss modeling. *Geosciences, 34*(1), 32–40.

Anjitha Krishna, P. R., Lalitha, R., Shanmugasundaram, K., & Nagarajan, M. (2019). Assessment of topographical factor (LS-Factor) estimation procedures in a gently sloping terrain. *Journal of the Indian Society of Remote Sensing, 47*, 1031–1039. https://doi.org/10.1007/s12524-019-00953-3

Ansari, A., & Tayfur, G. (2023). Comparative analysis of estimation of slope-length gradient (LS) factor for entire Afghanistan. *Geomatics, Natural Hazards and Risk, 14*(1), 2200890. https://doi.org/10.1080/19475705.2023.2200890

Aouichaty, N., Bouslihim, Y., Hilali, S., Zouhri, A., & Koulali, Y. (2022). Estimation of water erosion in abandoned quarries sites using the combination of RUSLE model and geostatistical method. *Scientific African, 16*, e01153. https://doi.org/10.1016/j.sciaf.2022.e01153

Arnoldus, HMJ (1977) Methodology used to determine the maximum potential average annual soil loss due to sheet and rill erosion in Morocco. *Assenssing soil degradation*, *Rome (Italy) FAO*.

Azizian, A., & Koohi, S. (2021). The effects of applying different DEM resolutions, DEM sources and flow tracing algorithms on LS factor and sediment yield estimation using USLE in Barajin river basin (BRB) Iran. *Paddy and Water Environment, 19*(3), 453–468. https://doi.org/10.1007/s10333-021-00847-6

Bols, P. (1978). The isoerodent maps of Java and Madura. *Belgican Technical Assistance Project ATA*, 105.

Brahim, B., Meshram, S. G., Abdallah, D., Larbi, B., Drisss, S., Khalid, M., & Khedher, K. M. (2020). Mapping of soil sensitivity to water erosion by RUSLE model: case of the Inaouene watershed (Northeast Morocco). *Arabian Journal of Geosciences, 13*(21), 1–15. https://doi.org/10.1007/s12517-020-06079-y

Dam Nguyen, D., Roussis, P. C., Thai Pham, B., Ferentinou, M., Mamou, A., Quang, Vu., D., et al. (2022). Bagging and multilayer perceptron hybrid intelligence models predicting the swelling potential of soil. *Transportation Geotechnics, 36*, 100797. https://doi.org/10.1016/J.TRGEO.2022.100797

Das, S., Bora, P. K., & Das, R. (2022). Estimation of slope length gradient (LS) factor for the sub-watershed areas of Juri River in Tripura. *Modeling Earth Systems and Environment, 8*(1), 1171–1177. https://doi.org/10.1007/s40808-021-01153-0

Desmet, P., & Govers, G. (1996). A GIS procedure for automatically calculatingthe USLE LS factor on topographically complex landscape units. *Journal of Soiland Water Conservation, 51*, 427–433.

Durigon, V. L., Carvalho, D. F., Antunes, M. A. H., Oliveira, P. T. S., & Fernandes, M. M. (2014). NDVI time series for monitoring RUSLE cover management factor in a tropical watershed.

International Journal of Remote Sensing, 35(2), 441–453. https://doi.org/10.1080/01431161.2013.871081

Escobar Quintero, J. N. (2021). Análisis comparativo entre rusle y el análisis multicriterio, para obtener la erosión hídrica en la microcuenca del río Amarillo, El Oro Ecuador [Bachelor's tesis]. *Facultad de Ciencias Naturales. Universidad de Guayaquil*.

Fayas, C. M., Abeysingha, N. S., Nirmanee, K. G. S., Samaratunga, D., & Mallawatantri, A. (2019). Soil loss estimation using rusle model to prioritize erosion control in KELANI river basin in Sri Lanka. *International Soil and Water Conservation Research, 7*(2), 130–137. https://doi.org/10.1016/j.iswcr.2019.01.003

Ganasri, B. P., & Ramesh, H. (2016). Assessment of soil erosion by RUSLE model using remote sensing and GIS—a case study of Nethravathi Basin. *Geoscience Frontiers, 7*(6), 953–961. https://doi.org/10.1016/j.gsf.2015.10.007

Ghosal, K., & Das Bhattacharya, S. (2020). A review of RUSLE model. *Journal of the Indian Society of Remote Sensing., 48*(4), 689–707. https://doi.org/10.1007/s12524-019-01097-0

Hui, L., Xiaoling, C., Lim, K. J., Xiaobin, C., & Sagong, M. (2010). Assessment of soil erosion and sediment yield in Liao watershed, Jiangxi Province, China, Using USLE, GIS, and RS. *Journal of Earth Science, 21*(6), 941–953. https://doi.org/10.1007/S12583-010-0147-4/METRICS

IDEAM. (2023). CLIMA ANALISIS CLIMATICO - GALERÍA DE MAPAS. http://www.ideam.gov.co/galeria-de-mapas/-/document_library_display/4VnjNLZDi78B/view/599272. Accessed 26 July 2023

Jazouli, A. E., Barakat, A., Khellouk, R., Rais, J., & Baghdadi, M. E. (2019). Remote sensing and GIS techniques for prediction of land use land cover change effects on soil erosion in the high basin of the Oum Er Rbia River (Morocco). *Remote Sensing Applications: Society and Environment, 13*, 361–374. https://doi.org/10.1016/j.rsase.2018.12.004

Karásek, P., Pochop, M., Konečná, J., & Podhrázská, J. (2022). Comparison of the methods for LS Factor calculation when evaluating the Erosion Risk in a small agricultural area using the USLE tool. *Journal of Ecological Engineering, 23*(1), 100–109. https://doi.org/10.12911/22998993/143977

Kidane, M., Bezie, A., Kesete, N., & Tolessa, T. (2019). The impact of land use and land cover (LULC) dynamics on soil erosion and sediment yield in Ethiopia. *Heliyon*. https://doi.org/10.1016/j.heliyon.2019.e02981

Koirala, P., Thakuri, S., Joshi, S., & Chauhan, R. (2019). Estimation of soil erosion in Nepal using a RUSLE modeling and geospatial tool. *Geosciences (switzerland)*. https://doi.org/10.3390/geosciences9040147

Lu, S., Liu, B., Hu, Y., Fu, S., Cao, Q., Shi, Y., & Huang, T. (2020). Soil erosion topographic factor (LS): accuracy calculated from different data sources. *CATENA, 187*, 104334. https://doi.org/10.1016/J.CATENA.2019.104334

Mallick, J., Alashker, Y., Mohammad, S. A. D., Ahmed, M., & Hasan, M. A. (2014). Risk assessment of soil erosion in semi-arid mountainous watershed in Saudi Arabia by RUSLE model coupled with remote sensing and GIS. *Geocarto International, 29*(8), 915–940. https://doi.org/10.1080/10106049.2013.868044

McCool, D. K., Brown, L. C., Foster, G. R., & Mutchler, C. K. (1987). Revised slope steepness factor for the Universal Soil Loss Equation. *Transactions of the ASAE (american Society of Agricultural Engineers), 30*, 1387–1396.

Menasria, A., Meddi, M., & Habaieb, H. (2022). Diachronic study of land cover of the Medjerda watershed and estimation of RUSLE-C Factor using NDVI-based equation, remote sensing, and GIS. *Journal of the Indian Society of Remote Sensing, 50*(3), 451–468. https://doi.org/10.1007/s12524-021-01472-w

Michalopoulou, M., Depountis, N., Nikolakopoulos, K., & Boumpoulis, V. (2022). The Significance of Digital Elevation Models in the Calculation of LS Factor and Soil Erosion. *Land*. https://doi.org/10.3390/land11091592

Mitasova, H., Hofierka, J., Zlocha, M., & Iverson, L. R. (1996). Modelling topographic potential for erosion and deposition using GIS. *International Journal of Geographical Information Systems, 10*(5), 629–641. https://doi.org/10.1080/02693799608902101

Mohammed, S., Alsafadi, K., Talukdar, S., Kiwan, S., Hennawi, S., Alshihabi, O., et al. (2020). Estimation of soil erosion risk in southern part of Syria by using RUSLE integrating geo informatics approach. *Remote Sensing Applications: Society and Environment*. https://doi.org/10.1016/j.rsase.2020.100375

Montanarella, L. (2015). Agricultural policy: govern our soils. *Nature, 528*(7580), 32–33. https://doi.org/10.1038/528032a

Moore, I. D., & Burch, G. J. (1986). Physical Basis of the Length-slope Factor in the Universal Soil Loss Equation. *Soil Science Society of America Journal, 50*(5), 1294–1298. https://doi.org/10.2136/SSSAJ1986.03615995005000050042X

Qiankun, G., Zhaowei, D., Wei, Q., Wenhong, C., Wen, L., Xiaomei, X., & Zhe, Y. (2019). Changes in sediment load in a typical watershed in the tableland and gully region of the Loess Plateau China. *CATENA*. https://doi.org/10.1016/j.catena.2019.104132

Renard, K. G., Foster, G. R., Weesies, G. A., McCool, D. K., & Yoder, D. C. (1997). *Predicting soil erosion by water a guide to conservation*. Washington: United States Department of Agriculture.

Schmidt, S., Tresch, S., & Meusburger, K. (2019). Modification of the RUSLE slope length and steepness factor (LS-factor) based on rainfall experiments at steep alpine grasslands. *MethodsX, 6*, 219–229. https://doi.org/10.1016/J.MEX.2019.01.004

Sinshaw, B. G., Belete, A. M., Mekonen, B. M., Wubetu, T. G., Anley, T. L., Alamneh, W. D., et al. (2021). Watershed-based soil erosion and sediment yield modeling in the Rib watershed of the Upper Blue Nile Basin Ethiopia. *Energy Nexus, 3*, 100023. https://doi.org/10.1016/j.nexus.2021.100023

Smith, D. D., & Wischmeier, W. H. (1957). Factors affecting sheet and rill erosion. *Eos, Transactions American Geophysical Union, 38*(6), 889–896.

Spanner, J., & Napolitano, G. (2015). Healthy soils are the basis for healthy food production. https://www.fao.org/soils-2015/news/news-detail/en/c/277682/. Accessed 25 November 2023

Van Oost, K., Govers, G., & Desmet, P. (2000). Evaluating the effects of changes in landscape structure on soil erosion by water and tillage. *Landscape Ecology, 15*(6), 577–589. https://doi.org/10.1023/A:1008198215674

Wang, G., Gertner, G., Parysow, P., & Anderson, A. (2001). Spatial prediction and uncertainty assessment of topographic factor for revised universal soil loss equation using digital elevation models. *ISPRS Journal of Photogrammetry and Remote Sensing, 56*(1), 65–80. https://doi.org/10.1016/S0924-2716(01)00035-1

Wischmeier, W. H., & Smith, D. D. (1978). Predicting Rainfall Eorsion Losses A guide to conservation planning. *Agriculture Handbook* 282. *USDA-ARS, USA*.

Xu, Z., Zhang, S., Zhou, Y., Hou, X., & Yang, X. (2022). Characteristics of watershed dynamic sediment delivery based on improved RUSLE model. *CATENA*. https://doi.org/10.1016/j.catena.2022.106602

Zhou, F. J., Chen, M. H., Lin, F. X., Huang, Y. H., & Lu, C. L. (1995). The rainfall erosivity index in Fujian Province. *Journal of Soil and Water Conservation, 1*, 13–18.